Research Square

Preprints are preliminary reports that have not undergone peer review.
They should not be considered conclusive, used to inform clinical practice,
or referenced by the media as validated information.

A transcriptome approach evaluating the effects of Atractylenolide Ⅰ on the secretion of estradiol and progesterone in feline ovarian granulosa cell

yuli guo
Inner Mongolia Agricultural University
Junping Liu
Inner Mongolia Agricultural University
Shuangyi Zhang
Inner Mongolia Agricultural University
Di Sun
Inner Mongolia Agricultural University
Zhiying Dong
Inner Mongolia Agricultural University
Jinshan Cao (6457304@qq.com)
Inner Mongolia Agricultural University

Research Article

Keywords: ovarian granulosa cell, Atractylenolide-Ⅰ, estradiol, progesterone, cholesterol metabolism

Posted Date: June 26th, 2023

DOI: https://doi.org/10.21203/rs.3.rs-3080498/v1

License: This work is licensed under a Creative Commons Attribution 4.0 International License.
Read Full License

Additional Declarations: No competing interests reported.

Abstract

Atractylodes macrocephala Koidz (AMK) as eartraditional oriental medicine has been used in the treatment of threatened abortion. *Atractylenolide I* (AT-I) is one of the major bioactive components of AMK. This study aimed to investigate the effect of AT-I on the secretion of estradiol (E_2) and progesterone (P_4) of feline ovarian granulosa cells (FOGCs) which is necessary for pregnancy. At first, the prolifeation of FOGCs after AT-I treatment was measured by CCK-8. Then, the synthesis of E_2 and P_4 were measured by ELISA. Lastly, transcriptome sequencing was used to detect the DEGs in the FOGCs, and RNA-Seq results were verified by RT-qPCR and biochemical verification. It was found that AT-I could promote proliferation and the secretion of E_2 and P_4 in FOGCs; after AT-I treatment, 137 significantly DEGs were observed, out of which 49 were up-regulated and 88 down-regulated. The DEGs revealed significant enrichment of 52 GO terms throughout the differentiation process ($P < 0.05$) as deciphered by Gene Ontology enrichment analysis. Kyoto Encyclopedia of Genes and Genomes analysis manifested that the DEGs were successfully annotated as members of 155 pathways, with 23 significantly enriched ($P < 0.05$). A relatively high number of genes were enriched for the cholesterol metabolism, ovarian steroidogenesis, and biosynthesis of unsaturated fatty acids. Furthermore, the contents of the total cholesterol and low-density lipoprotein cholesterol were decreased by AT-I treatment in the cell culture supernatant. The results indicated that AT-I could increase the ability of FOGCs to secrete E_2 and P_4, which might be achieved by activation of cholesterol metabolism.

1. Introduction

Atractylodes macrocephala Koidz (AMK) has been commonly used in the clinical prescription for preserving fetuses, and their fetal safety effects have been confirmed by thousands of years of medical practice in traditional Chinese medicine (Zhu et al., 2018). As one of the major bioactive components in AMK, *Atractylenolide I* (AT-I) is a naturally occurring sesquiterpene lactone has been found to display a wide range of pharmacological and biological activities such as anti-atherosclerotic and the treatment of various inflammatory illness, etc (G. Ji, 2014; Li et al., 2017; Long et al., 2017; Song et al., 2017).

The Progesterone (P4) has a variety of physiological functions, such as promoting endometrial decidualization,establishing maternal-fetal immune tolerance,inhibiting inflammatory response, and improving uterine-placental circulation, which are prerequisites for the maintenance of pregnancy (Mesen and Young, 2015; Nardo and Sallam, 2006). Insufficient secretion of P_4 affects endometrial secretion, thereby affecting embryo implantation and development. In early embryonic development, P_4 mainly comes from luteal granulosa cells, so the activity of granulosa cells plays a very important role in corpus luteum (CL) development and early pregnancy maintenance (Niswender et al., 2000). Maintaining a certain concentration of estradiol (E_2) can increase the uterine placental blood flow and increase the sensitivity of the uterus to P_4 (Braun et al., 2012).E_2 plays a role in the endometrium mainly through its homologous nuclear receptors ESR1 and ESR2, and participates in the decidualization process of the endometrium through the ERK/MAPK pathway (Braun et al., 2012). Studies have shown that if the E_2

content is too low, it would lead to embryo implantation failure (Vannuccini et al., 2016). Therefore, determining the effect of AT-I on the secretion of E_2 and P_4 in feline ovarian granulosa cells (FOGCs) might contribute to our understanding of the protection of AMK in early pregnancy.

In recent years, the high-throughput RNA sequencing technique (RNA-seq) has emerged as a powerful tool for transcriptome analysis (Guo-Liang Zhang, 2017). By using this method, it might help to assess the changes of the transcriptome in FOGCs upon treatment with AT-I at the whole genome scale, contributing to explain the mechanism of how AT-I regulates the changes of FOGCs.

2. Materials and methods

2.1 AT-I structure

AT-I (CAS No. 73069-13-with purity ≥ 98%) used in this study were purchased from Dalian Meilune Biotechnology Co. Ltd. (Liaoning, China). The chemical structure of the AT-I has been depicted in Fig. 1.

2.2 Culture of primary feline ovarian granulosa cells

FOGCs were obtained from fresh ovarian tissues of healthy and diestrus period felines between six months and two years old, which were under sterilization operation in the animal hospital of Inner Mongolia Agricultural University. The feline ovarian tissues were maintained in a vacuum thermos flask containing sterile physiological saline and transported to the laboratory within 2 h. The ovarian tissues were washed several times with 37 ℃ DPBS solution (Gibco, MA, USA), contained 3% penicillin and streptomycin (Gibco, MA, USA,) until the tissues completely clean. The tissues were then transferred to a 300 mm diameter plate with 0.5 mL of 12% fetal calf serum-supplemented Ham's F-12 nutrient mixture (DMEM/F12, Gibco, MA, USA). Thereafter, the follicular fluid and cumulus-oocyte complexes (COCs) from primary follicles between 1 and 1.5 mm in diameter were aspirated by using a 2.5 mL aseptic syringe. Collected cells were transferred to a 1mL centrifuge tube and centrifuged at 1500 rpm for 3 min, then sediment was harvested and washed with DPBS solution. This process was repeated three times. Afterward, the isolated FOGCs were transferred in DMEM/F12 medium containing 12% fetal bovine serum (Excell Biology, Shanghai, China), 1% streptomycin and penicillin, and cultivated in a 5% CO_2 incubator at 37°C. Cell growth and morphological characteristics were observed with inverted microscope (Philips, Tokyo, Japan). After 72 h, the oocytes were washed out with DPBS, and the granulosa cells were isolated. Then, the medium was renewed routinely every other day until the cell density reached 75–80%, then digested with 0.25% trypsin-EDTA (Gibco, MA, USA) of 1mL for 2 min, and the digestion was terminated with the DMEM/F12 culture medium containing 12% serum. After fully mixing, inoculated at a split ratio of 1:2 for subsequent cultivation.

2.3 Morphological observations

The FOGCs at the logarithmic growth phase were seeded 100 μL at a density of 1×10^5 cells/mL on the autoclaved slides, thereafter the slides were stored in an autoclaved wet box that was placed in a 37°C,

5% CO_2 incubator for 24 h. After reaching 70% confluence, washed three times with DPBS and the cells were fixed for 20 min with cold acetone. The processed slides were then stained with two different staining methods: hematoxylin-eosin (HE) and Wright-Giemsa, photographed and analyzed by using a light microscope (ECLIPSE TS100-F. Nikon, Tokyo, Japan).

2.4 Immunofluorescence identification

To analyze the identity and purity of isolated FOGCs, immunofluorescence staining for a specific marker of ovarian granulosa cells was performed by FSHR (follicle stimulating hormone receptor). Seeded the logarithmic growth phase FOGCs 0.5 mL at a density of 1×10^5 cells/mL into 35 mm glass-bottom dishes (Shengyou Biotechnology, Hangzhou, China). After the cells reached 80% confluence, washed three times with aseptic DPBS solution, fixed for 30 min with 4% paraformaldehyde (Solarbio, Beijing, China) at room temperature, and washed three times with DPBS. After fixation, the FOGCs were incubated with 1mL 0.25% Triton X-100 (PH=7.40, Sigma-Aldrich, MO, USA) for 20 min, then washed three times with DPBS. After blocking for non-specific binding sites, the cells were stained with primary antibody to FSHR (1:200, Rabbit Anti-FSH receptor antibody; BS-0895R; Bioss; Beijing, China) overnight at 4°C. The granulosa cells were washed three times in DPBS and incubated with a secondary antibody (Alx647; donkey-anti-rabbit IgG; Jackson, Pennsylvania, USA) for 2 h at room temperature in the dark. After incubation, the cells were washed three times for 10 min with DPBS in the dark. Then with DAPI stained the nuclei, washed on the decolorizing shaker 4 times for 10 min. Observed glass-bottom dishes under an LSM 800 (Zeiss, Jena, Germany) laser confocal system.

2.5 Cell viability assay

The cell viability was assessed using Cell Counting Kit-8 assays (CCK-8; BS350B; Biosharp; Shanghai, China). The second-generation feline ovary granule cells were used, washed with DPBS, and 1mL of 0.25% trypsin–EDTA was added to digest them for 2 min. Thereafter, DMEM/F12 medium containing 12% fetal bovine serum (Excell Biology, Shanghai, China) was added to stop the digestion. The pipetting was repeated to ensure that the cells are away from the wall and uniformly distributed. After digestion, the cell suspension concentration was adjusted to 2×10^6 cells/mL. Thereafter, a 96-well cell culture plate was taken, 100 μL of culture medium with cells was added to each well, and the plate was incubated for 12 h. Thereafter, 100 μL DPBS was added to the remaining wells to reduce evaporation. The cells in the plate were purified for 6 h (with the serum-free medium), the cell supernatant was purged after purification, and 100 μL medium (containing 12% serum) was added. The plate was cultivated for 6 h, 12 h, 24 h, 36 h, and 48 h, then CCK-8 was added for 4 h. After then, the absorbance value (OD value) of each well was measured with a microplate reader at a wavelength of 450 nm.

2.6 Cytotoxicity of AT-Ⅱ against primary feline ovarian granulosa cells

After the FOGCs purified as described above, 100 μL medium (containing 12% serum) with different AT-I concentrations (0 μmol/L, 1 μmol/L, 3 μmol/L, 10 μmol/L, 30 μmol/L, 100 μmol/L, 300 μmol/L) was

added to the plate and incubated at 37℃ for 0 h,12 h, 24 h, 36 h and 48 h, CCK-8 was added for 4 h and the absorbance value of each well was measured with a microplate reader at a wavelength of 450 nm to measure the cytotoxicity.

2.7 Determination of estradiol (E_2) and progesterone (P_4) concentration

FOGCs were seeded at a density of 2×10^6 cells/mL in 6-well cell culture plates and cultivated at 5% CO_2 and 37°C until 70% of the cells were fused. The cell culture supernatant was then removed and 2 mL of fresh DMEM/F12 medium containing 10 μmol/L AT-I was added to the FOGCs monolayer for co-culturing at 37°C with 5% CO_2. After incubation for 0 h, 12 h, 24 h, 36 h and 48 h respectively, the supernatant was aspirated and used for subsequent experiments. The control cells were treated with DMEM/F12 medium with the same time condition. Three different biological replicates were designed for both the treatment and control experiments.

The concentrations of E_2 in the culture medium were measured by enzyme-linked immunosorbent assay (Wuhan Xinqidi Biological Technology; Wuhan, China) according to the manufacturer's instructions. The estradiol standard curve ranged from 0 to 1000 pg/mL. The samples were analyzed in triplicates. The assay sensitivity, range, and intra-assay coefficient of variation were 5 pg/mL, 15.6–1000 pg/mL, and ≤ 8%, respectively. The concentrations of P_4 in the culture medium were measured by enzyme-linked immunosorbent assay (Wuhan Xinqidi Biological Technology; Wuhan, China) according to the manufacturer's instructions. The progesterone standard curve ranged from 0 to 100 ng/mL. The samples were analyzed in triplicates. The assay sensitivity, range, and intra-assay coefficient of variation were 0.5 ng/mL, 1.56–100 ng/mL, and ≤ 8%, respectively.

2.8 AT-I treatment

According to the above experiments, we selected the 10 μmol/L AT-I and incubated it for 36 h for the next study. FOGCs were seeded at a density of 2×10^6 cells/mL in 6-well cell culture plates and cultivated at 37°C and 5% CO_2 until they reached 70% confluence. The cell culture supernatant was thereafter removed and 2 mL of fresh DMEM/F12 medium containing 10 μmol/L AT-I was added to the FOGCs monolayer and the plate was incubated for 36 h at 37°C and 5% CO_2. After AT-I treatment, FOGCs were photographed and analyzed for potential morphological changes using an inverted microscope (Philips, Tokyo, Japan). The supernatant was aspirated and used for subsequent experiments. Thereafter, FOGCs were gently washed three times with DPBS to remove the remaining drug, collected the cells for transcription analysis. The control cells were treated with DMEM/F12 medium only. Three biological replicates were tested for the treatment and control experiments.

2.9 RNA library construction and sequencing

Total RNA from untreated and AT-I treated FOGCs was extracted according to the instructions of the Axygen-RNA extraction kit (AxyGen, CA, USA), and there were three biological repeats in each group.

Bioanalyzer 2100 and RNA 6000 Nano LabChip Kit (Agilent, CA, USA) were thereafter used to analyze the quantity and purity of total RNA, yielding RIN scores>8.0, in accordance with the testing standard. Magnetic beads connected with Oligo were used to enrich and purify eukaryotic mRNA with poly-A tail. The extracted eukaryotic mRNA was randomly broken into short fragments by the fragmentation reagent (Fragmentation Buffer). Using the fragmented mRNA as the template, one-strand cDNA was synthesized by a six-base random primer (Random hexamers), and then the buffer, dNTPs, RNaseH, and DNA Polymerase I was added to synthesize the two-strand cDNA. The cDNA double-stranded product was purified by AMPureXP beads. The viscous end of DNA was repaired to a flat end by T4 DNA polymerase and Klenow DNA polymerase, and the 3 'end was selected by adding base An and splice, AMPureXP beads. Finally, the final sequencing library was obtained by PCR amplification. After passing the quality inspection of the library, the library was sequenced with Illumina Hiseq 4000 to produce 150 bp double-terminal data. The cDNA library was sequenced on an Illumina HiSeq 4000 sequencing platform (Illumina, San Diego, USA) provided by Majorbio Bio-pharm Technology Co., Ltd (Shanghai, China).

2.10 Statistical analysis of transcription data

The raw RNA-seq data was then filtered to remove various adaptor contamination, low-quality bases, and undetermined bases utilizing Cutadapt software (Maher et al., 2009). The sequencing quality was verified using FASTQC software including the Q20, Q30, and GC content of the clean data. All downstream analysis was based on clean as well as high-quality data. The filtered reads were aligned and mapped to the reference genome using Hisat 2.0. The aligned read files were processed by Cufflinks (Martin M, 2011), which uses the normalized RNA-seq fragment counts to measure the relative abundances of the different transcripts. The unit of measurement is fragments per kilobases of exon per million fragments mapped (FPKM). The DEGs were screened using R package edger (Love M I, 2014) with fold change (FC) ≥ 1.5 and *P-adjust*<0.05, which were considered significantly different expressed (Anders and Huber, 2010). The DEGs underwent enrichment analysis using GO and KEGG. *P* values were calculated using the Benjamini-corrected modified Fisher exact test, and *P*<0.05 was deemed statistically significant.

2.11 Validation by quantitative reverse transcription PCR

Quantitative reverse transcription PCR (RT-qPCR) was utilized to validate the DEGs identified by RNA-seq. The total RNA concentration of all samples was adjusted to 300 ng/μL at the same time, and cDNA was used as starting material for real-time PCR with FastStart Universal SYBR Green Master (Roche, Mannheim, Germany) on an iQ5 multicolor real-time PCR detection system (Bio-Rad, CA, USA). Eight DEGs were chosen based on changes in their expression levels in the treated cells as compared with the control cells. Eight DEGs were selected with cDNA as template and the glyceraldehyde 3-phosphate dehydrogenase (*GAPDH*) gene was used as the internal control. The sequence of primers is shown in Table 3. The RT-qPCR reaction conditions are as follows: 5 min pre-incubation at 95°C; 40 cycles of amplification for 5 s at 95°C for denaturation, 34 s at 60°C for annealing, and 20 s at 72°C for elongation. Negative controls (without cDNA) were run in the same reaction set. The relative mRNA expression of DEGs in each group was calculated by the $2^{-\Delta\Delta Ct}$ formula (Kanehisa et al., 2008).

2.12 Biochemical verification

After 10 μmol/L AT-I treatment for 36 h, the supernatant was collected for biochemical testing (Inc.BS-180vet blood biochemical analyzer; Abaxis, USA). Three biological replicates were used for the treatment and control experiments. The contents of total cholesterol (TC) and low-density lipoprotein cholesterol (LDL-C) in the supernatant were detected to explore the possible effect of AT-I on lipid metabolism.

2.13 Statistical analysis

The experimental data were expressed as mean ± SD. The difference between the two groups was analyzed using the T-test and One-way ANOVA. $P < 0.05$ was considered significant with *, $P < 0.05$ and **, $P < 0.01$.

3. Results

3.1 Identification of cultured feline ovarian granulosa cells

The cells nearby the oocytes begun to display an elongated or fibroblastic property within the first 36 h (Fig. 2A). The cells were then distinguished by the presence of a triangle cone or irregular star-shaped morphology. After 3 days of culture, large number of cells was observed around oocytes in clusters. The cells confluence reached 75 to 80% on day 7. The sub-cultured cells began to adhere after 4 h, the cell could reached to 80% confluence on day 3. The similar phenomenon happed on passages 3 and 4 with classic irregular star-shaped morphology.

By HE staining, the structure of cells was confirmed to be contact by which the edge was clear and a triangle cone or irregular star shape. The cytoplasm was pink, and the nuclei were dyed in blue (Fig. 2C). By Giemsa staining, the structure of cells also presented contact by which the edge was clear and a triangle cone or irregular star shape. The cytoplasm was blue-violet and the nuclei were pink (Fig. 2D).

The FSHR was expressed in the cytoplasm of triangle cone-like cells by immunofluorescence staining, while FSHR was not observed in control group (without primary antibody) (Fig. 2E), confirming that FOGCs were cultivated successfully and the purity could reach 90%.

3.2 Cell viability assay

The cell growth curve detected by CCK-8 assay (Fig. 2B) showed that cell proliferation significantly happened after 12 h until 48 h ($P < 0.05$), indicating that the way of cultivated FGOCs growth consist with that in normal cell growth.

3.3 Cytotoxicity of AT- on the primary FOGCs

AT-I treatment in a concentration range (0 μmol/L-300 μmol/L) showed that 1, 3, 10 and 30 μmol/L could effectively promote FOGCs proliferation from 12 h to 48 h (Fig. 3A). 100 μmol/L significantly increased FOGCs proliferation after 36 h and the increased effect of 300 μmol/L happened at 48 h ($P < 0.05$) (Fig. 3A). In addition, under the microscope, the increased density of granulosa cells by 10 μmol/L AT-I

treatment for 36 h was clearly observed as well (Fig. 3B). These results indicated that the 10 μmol/L AT-I could enhance the viability at 36 h most obviously among selected concentration and time points indicating 10 μmol/L could be used as the experimental concentration for following experiment.

3.4 The effect of AT-I on the synthesis of E_2 and P_4 in FOGCs

10 μmol/L AT-I could significantly promote the E_2 secretion in FOGCs at 24 h and 36 h, while the increased tendency weakened at 48 h (Fig. 4A). The P_4 concentration significantly increased by AT-I treatment from 12 h to 48 h (Fig. 4B). Although the secretion of E_2 and P_4 was both increased, the ratio of P_4/E_2 indicated that the E_2 secretion was more obviously than P_4 secretion in FOGCs within 36 h after AT-I treatment. However, the secretion pattern of E_2 and P_4 changed at 48 h, in which the FOGCs secret P_4 more obviously than that E_2 secretion(Fig. 4C).

3.5 Classification of transcriptional sequencing data

To evaluate the transcriptional response of the FOGCs to AT- exposure and decipher the various host factors, which may be involved in the luteinization, the Illumina HiSeq 4000 platform with cDNA libraries of FOGCs treated with AT- were used. The sequencing quality data are shown in Table 1, the two libraries produced 58,841,865 and 52,950,059 original sequences (Raw Data), respectively, from both the treated and control FOGC groups. After filtering, the effective date of 58,189,124 and 52,340,848 was obtained. The proportion of data quality Q20 (sequencing base mass) of the two databases is more than 98%, which meets the needs of follow-up test analysis. All the valid reads were aligned to the feline genome using Hisat 2.0. Furthermore, 56,730,426 and 51,014,192 Map Reads were obtained from the different groups of treated and control FOGCs, in which the number of Reads with unique alignment position in the genome and meeting the needs of subsequent experimental analysis were 53,563,083 and 48,058,826 respectively, and the ratio of alignment to genome sequence was 92.06% and 91.82%, respectively. The results show that the sequencing data are of high quality and meet the needs of further analysis.

The sequencing data have been saved in the NCBI gene expression comprehensive database (http://www.ncbi.nlm.nih.gov/geo/info/linking.html) and can be obtained by GEO Series accession number GSE155784.

3.6 Analysis of differentially expressed genes

FOGCs treated with the AT- showed a relative degree of differential expression. A total of 137 DEGs were obtained (≥ 1.5-Fold Change, *P-adjust* < 0.05), of which 49 DEGs were significantly up-regulated and 88 DEGs were significantly down-regulated. The overall distribution of DEGs can be understood by drawing a volcanic map. (Fig. 5).

3.7 Functional enrichment analysis of differentially expressed gene

The RNA-seq analysis revealed a total of 17 265 genes, of which 137 genes were significant differences in expression. To assess the biological functions of the 137 DEGs, enrichment analysis of GO classification (http://www.geneontology.org/) and the KEGG pathway (http://www.genome.jp/kegg) was systematically performed. The annotated results of the GO database in the sequencing are shown in Fig. 6. The histogram of GO enrichment analysis is mainly reflected in biological processes, cellular components, and molecular functions. In biological processes, 644 DEGs are assigned to the regulation of biological processes, such as cellular processes, single-organism process, biological regulation, regulation of biological process development, and metabolic processes. In the cell component field, 308 DEGs belong to the the cell, the cell part, and membrane. In the molecular functional class, 93 DEGs resins can be used for binding and catalytic activity.

KEGG analysis showed that the DEGs were mainly involved in the regulation of the various signal transduction pathways, signaling molecules and their possible interactions, membrane transport, lipid metabolism, endocrine system, as well as digestive system (Fig. 7). The DEGs successfully annotated 155 signal pathways, and 23 signal pathways were significantly different ($P < 0.05$). Relatively high numbers of different genes were involved in the regulation of cholesterol metabolism, ovarian steroidogenesis, rheumatoid arthritis, biosynthesis of unsaturated fatty acids, steroid hormone biosynthesis, AMPK signaling pathway, ABC transporters, and other signaling pathways (Fig. 8).

DEGs were analyzed with KEGG to predict and study the signal pathways that are mainly involved and most interested, and to obtain those pathways that may be related to the luteinizing effect of AT-I. In the various pathways associated with the response of the FOGCs treated with AT-I, 9 DEGs were found to be significantly affected (Table 2). Among the DEGs, three genes (*ABCA1*, *LDLR*, and *SREBF1*) were found to be upregulated and involved in the regulation of the cholesterol metabolism, cholesterol metabolism is a complex biological process and most of the other DEGs identified were also found to actively participate in this process. Three genes (*StAR, LDLR* and *CYP1A1*) have been implicated in the regulation of ovarian steroidogenesis. Two genes (*SCD*, and *FADS2*) were upregulated and were found to be involved in the biosynthesis of unsaturated fatty acids. Two genes (*ABCG1*, and *ABCA1*) were upregulated and participated in ABC transporters, and the two DEGs (*SREBF1*, and *SCD*) were observed to be upregulated and could participate in the regulation of the AMPK signaling pathway.

3.8 Validation of the selected Genes by quantitative reverse transcription PCR and Biochemical analysis

To validate the results of RNA-seq analysis, RT-qPCR was used to examine the various DEGs. All DEGs have the same trend of changes with RNA-seq data. Thereby suggesting that the RNA-seq data reliably reflected the changes in the trends of gene expression (Fig. 9A).

To verify whether AT-I can promote the metabolism of cholesterol, the biochemical analysis of the supernatants of granulosa cells treated with AT-I was carried out. It was found that the contents of the

total cholesterol (TC) and low-density lipoprotein cholesterol (LDL-C) in the treated group with AT-I were significantly lower than those in the control group (Fig. 9B).

4. Discussion

AT-I has been found to be the the major bioactive component from AMK, which is a medicinal plant that has been used as a pharmacological agent for the treatment of threatened miscarriages for a long time (Zhu et al., 2018). CL is an essential organ for maintain the early pregnancy, and luteal dysfunction could cause infertility and abortions (Mesen and Young, 2015). The CL is mainly composed of large luteum cells (LLC) and little amount of small luteum cells (SLC). LLC, which has the stronger steroidogenic capacity than that in SLC, mainly originates from ovarian granulosa cells (Hryciuk et al., 2019). As the major bioactive compent of AMK, the effect of AT-I on the ovarian granulosa cells might contribute to our understanding on how AMK treatment of threatened miscarriages. This study found that AT-I could promote proliferation and the secretion of E_2 and P_4 in FOGCs. And the transcriptome profile of differential gene expression in FOGCs treated with the AT-I was examined in this report.

Ovarian granulosa cells as the largest cell group within the follicles, they not only cooperate with theca interstitial cells to regulate the synthesis of female steroid hormones, and also can regulate both the growth and maturation of oocytes (Havelock et al., 2004). At present, there is only one method to culture primary FOGCs by slicing ovaries into many pieces (Chiara Perego et al., 2021), but the cell identification was not carried out and the fibroblasts, endothelial cells could not effectively removed. In this study, a new method by puncturing small folliclesto to cultivate primary FOGCs and confirmed with FSHR immunofluorescence identification, the FOGCs purity could reach 90% which could be used to perform relative experiment.

After ovulation, ovarian granulosa cells proliferation and transformed to LLC that can have the ability to secrete amount of P_4 and maintain early pregnancy (Luigi Devoto, 2009) (Richards and Pangas, 2010); Amelkina et al. revealed that ovarian granulosa cells could be transformed to LLC that can have the ability to secrete steroids in domestic cat (Amelkina et al., 2015). In this study, the FOGCs viability was noticed to increase significantly in a dose and time-dependent within a certain range (Fig. 3A and 3B) and the secretion of E_2 and P_4 increased significantly (Fig. 4) after AT-I treatment in FOGCs. The increase of E2 and P4 might due to cell proliferation or enhanced single cell secretion or combined effect, which needs further investigation.

Recent evidence obtained with a luteal cell line has confirmed that E_2 can positively regulate the transcriptional activity of the *SR-BI* gene to speed up the occurrence of the luteinization process (Stocco, 2007). In our study, after AT-I-stimulation, E_2 concentration was observed to increase in 36 h, and after AT-I treatment 36 h, FOGCs can produce a substantial amount of P_4 instead of E_2 that they did before and the ratio of P_4/E_2 indicated that the P_4 secretion was more obviously than E_2 secretion in FOGCs after 36 h indicating that the AT-I might initiate luteinization process, which resulted in the enhanced P_4 secretion in FOGCs .

In this study, a total of 137 DEGs were obtained after transcriptome sequencing on the FOGCs group treated with AT-I and these results were confirmed by RT-qPCR. According to the GO classification and KEGG pathway enrichment analysis, it was found that the DEGs were mainly enriched in several important pathways including those regulating cholesterol metabolism, ovarian steroidogenesis, biosynthesis of unsaturated fatty acids and ABC transporter.

The unsaturated fatty acids are able to reduce the harmful cholesterol and triglyceride in the blood by esterifying cholesterol and promote cholesterol metabolism effectively control the concentration of blood lipids, and increase the content of high-density lipoprotein (HDL) which is beneficial to the human body (Wiktorowska-Owczarek et al., 2015). The DEGs *SCD*, a central regulator controlling the biosynthesis of unsaturated fatty acids (AM et al., 2017) was up-regulated by AT-I which might contribute to the secretion of E_2 and P_4 through regulate the biosynthesis of unsaturated fatty acid.

The cholesterol metabolism is critical for the production of the various essential membrane components which is necessary for cell proliferation (Miranda-Jimenez and Murphy, 2007). In addition, as a precursor of steroid hormones, cholesterol is pivotal for ovarian follicular maturation (Shimano and Sato, 2017). Interestingly, in this study, it was found that the DEGs after AT-I treated mainly related to cholesterol metabolism. A constant supply of cholesterol is needed for the synthesis of steroid hormones in the CL and maternal cholesterol metabolism plays a role in fetal development (Woollett, 2008). Circulating plasma lipoproteins are the major source of cholesterol for steroid production in these different cells and cholesterol can be mainly obtained from circulating low-density lipoproteins (LDL) and small part from high-density lipoprotein (HDL) (Li et al., 2019; Miranda-Jimenez and Murphy, 2007). There are multiple systems involved in the cellular cholesterol delivery for steroidogenesis, mainly through the uptake of lipoprotein-derived cholesterol via LDLR mediated endocytic pathways (Craig et al., 2011). According to the RNA-seq analysis and RT-qPCR result, the expression of *LDLR* was induced by AT-I treatment in FOGCs, indicating the uptake of lipoprotein-derived cholesterol might be activated which could further stimulate the cholesterol biosynthesis.The identified DEGs *SREBF1* that responsible for encoding sterol regulatory element-binding protein (SREBP) able to promote the transcription of various lipogenesis involved in the biosynthesis of fatty acids and cholesterols and involved in the regulation of sterol synthesis rates (Richards and Pangas, 2010; Wang et al., 2020; Woollett, 2008). It was reported that SREBP could up-regulated the LDLR expression promote the cholesterol uptake (Lindholm et al., 2009; Shimano and Sato, 2017) and regulate the luteinization process through enhance the sensitivity of Human Granulosa-Lutein Cells to LH (Li et al., 2019). After AT-I treatment, the *SREBF1* expression was up-regulated than that in control group, suggesting the SREBF1 signaling pathway might be activated. The activation of SREBF1 signaling pathway by AT-I treatment might contribute to the FOGCs synthesis of steroid hormones.To further confirm the effect of AT-I on cholesterol metabolism, the biochemical test was used to detect the content of cholesterol in the cell supernatant. After AT-I treatment 36 h, the contents of total cholesterol and LDL cholesterol both declined, whereas the synthesis of steroid hormones increased, suggested that AT-I indeed significantly affect cholesterol metabolism and promote the secretion of E_2 and P_4 in FOGCs. Li et al showed that AT-I dose dependently inhibited Ox-LDL induced

VSMCs proliferation to treat atherosclerosis (Li et al., 2017), which might be the result of increased LDLR expression.

The ovaries are responsible for producing sex steroid hormones during reproductive life, which is important for both reproductive and somatic health (Richards and Pangas, 2010). After AT-I treatment, the secretion of E_2 and P_4 increased significantly in FOGCs. The *CYP1A1* was down-regulated and thereby can reduce the degradation of E_2 to modulate ovarian steroidogenesis (Deok-Soo Son 1999). The identified DEGs *LDLR* is also a key gene in ovarian steroidogenesis by promote the cholesterol biosynthesis. The DEGs *StAR* can introduce cholesterol into mitochondria, which is essential for steroid production. Cholesterol is the major raw material for ovarian steroid hormone synthesis. According to this study, the expression of *LDLR,StAR* and *SREBF1* increased were induced by AT-I treatment in FOGCs, and the increased gene might further stimulate the cholesterol biosynthesis which leading ovarian steroidogenesis happened.

The *ABCA-1* and *ABCG-1* expression increased after AT-I treatment might improve the reverse cholesterol transport, and further speed up the metabolic process of cholesterol in FOGCs since ABC transport system can drive intracellular superfluous cholesterol from arterial wall macrophages to the liver, thus allowing its excretion into the bile and feces as to speed up the metabolic process of cholesterol (Iborra, 2011).

AT-I can promote the biosynthesis of unsaturated fatty acids to enhance the HDL content in plasma, and dramatically enhance the ability to transport LDL into cells by increased *LDLR* expression; The intake cholesterol can be used as raw material for ovarian steroidogenesis incloud E_2 and P_4. At the same time, AT-I can dynamically promote the reverse transport of cholesterol by up-regulating *ABCA1* and *ABCG-1* gene expression to speed up the metabolic process of cholesterol. Taken together, after AT-I treatment, the differential genes identified were mainly concentrate on cellular cholesterol uptake and efflux. Thus, it was hypothesized that AT-I might affect the secretion of E_2 and P_4 by promoting the cholesterol metabolism in the granulosa cells.

5 Conclusion

This study demonstrated that AT-I could promote cholesterol metabolism determined by RNA-seq and biochemical test in FOGCs. The effect of AT-I on cholesterol metabolism might help to explaining the AT-I induced the secretion of E_2 and P_4 in FOGCs. These results together will contribute to our understanding of the mechanism of early pregnancy protection by AMR.

Abbreviations

AMK *Atractylodes macrocephala Koidz*

AT-I *atractylenolide I*

FOGCs primary feline ovarian granulosa cells

RNA-seq transcriptome sequencing

CL corpus luteum

LLC large luteum cells

SLC small luteum cells

E_2 estradiol

P_4 progesterone

ELISA enzyme linked immunosorbent assay

DEGs differentially expressed genes

GO Gene Ontology

KEGG Kyoto Encyclopedia of Genes and Genomes

FC fold change

FPKM fragmented per kilobases of exon per million fragments mapped

RIN RNA integrity number

RT-qPCR quantitative reverse transcription PCR

DPBS dulbecco's phosphate-buffered saline

DMEM/F12 Ham's F-12 nutrient mixture

COCs cumulus-oocyte complexes

HE hematoxylin-eosin

FSHR follicle stimulating hormone receptor

DAPI 4,6-diamidino-2-phenylindole

CCK-8 cell counting kit 8

OD value optical density value

TC total cholesterol

LDL-C low density lipoprotein cholesterol

HDL-C high density lipoprotein cholesterol

SD standard deviation

Declarations

Acknowledgments

This work was supported by the National key research and development plan "New technology for diagnosis, treatment, and prevention of pet diseases Research" (Grant 2016YFD0501000).

All data included in this study are available upon request by contact with the corresponding author.

The authors would like to thank Shanghai Majorbio Bio-pharm Technology Co., Ltd for sequencing services.

Author contributions: Y.L Guo carried out the study, analyzed, and interpreted the data and compiled the article. J.P Liu, S.Y Zhang contributed to the design of the study, discussion of the results, and critical revision of the article. Z.Y Dong, Sun contributed to the hormone analysis and critical revision of the article. J.S Cao supervised the study and contributed to its design, discussion of the results, and critical revision of the article.

Ethics approval

All animal studies were conducted in accordance with the experimental practices and standards approved by the Animal Welfare and Research Ethics Committee at Inner Mongolia Agricultural University (Approval ID: 20160829-1).

Declaration of competing interest

The authors declare that there is no conflict of interest.

References

1. AM, A.L., Syed, D.N., Ntambi, J.M., 2017. Insights into Stearoyl-CoA Desaturase-1 Regulation of Systemic Metabolism. Trends Endocrinol Metab 28(12), 831-842.https://doi.org/10.1016/j.tem.2017.10.003
2. Amelkina, O., Braun, B.C., Dehnhard, M., Jewgenow, K., 2015. The corpus luteum of the domestic cat: histologic classification and intraluteal hormone profile. Theriogenology 83(4), 711-720.https://doi.org/10.1016/j.theriogenology.2014.11.008

3. Anders, S., Huber, W., 2010. Differential expression analysis for sequence count data. Genome Biol 11(10), R106.https://doi.org/10.1186/gb-2010-11-10-r106
4. Braun, B.C., Zschockelt, L., Dehnhard, M., Jewgenow, K., 2012. Progesterone and estradiol in cat placenta–biosynthesis and tissue concentration. J Steroid Biochem Mol Biol 132(3-5), 295-302.https://doi.org/10.1016/j.jsbmb.2012.07.005
5. Chiara Perego, M., Bellitto, N., Maylem, E.R.S., Caloni, F., Spicer, L.J., 2021. Effects of selected hormones and their combination on progesterone and estradiol production and proliferation of feline granulosa cells cultured in vitro. Theriogenology 168, 1-12.https://doi.org/10.1016/j.theriogenology.2021.03.017
6. Craig, Z.R., Wang, W., Flaws, J.A., 2011. Endocrine-disrupting chemicals in ovarian function: effects on steroidogenesis, metabolism and nuclear receptor signaling. Reproduction 142(5), 633-646.https://doi.org/10.1530/Rep-11-0136
7. Deok-Soo Son , K.U., Xin Gao, Christopher C. Taylor ,Katherine F. Roby, Karl K. Rozmane, Paul F. Terranova,, 1999. 2,3,7,8-Tetrachlorodibenzo-p-dioxin (TCDD) blocks ovulation by a direct action on the ovary without alteration of ovarian steroidogenesis: lack of a direct effect on ovarian granulosa and thecal-interstitial cell steroidogenesis in vitro. Reproductive Toxicology 13, 521–530
8. G. Ji, R.C., J. Zheng, , 2014. Atractylenolide I inhibits lipopolysaccharide-induced inflammatory responses via mitogen-activated protein kinase pathways inRAW264.7 cells. Immunotoxicol. 36 (2014) 420–425.https://doi.org/10.3109/08923973.2014.968256
9. Guo-Liang Zhang, R.-Q.Z., Wei Shen and Lan Li, 2017. RNA-seq based gene expression analysis of ovarian granulosa cells exposed to zearalenone in vitro: significance to steroidogenesis. Oncotarget Vol. 8, 64001-64014.https://doi.org/https://doi.org/10.18632/oncotarget.19699.
10. Havelock, J.C., Rainey, W.E., Carr, B.R., 2004. Ovarian granulosa cell lines. Mol Cell Endocrinol 228(1-2), 67-78.https://doi.org/10.1016/j.mce.2004.04.018
11. Hryciuk, M.M., Braun, B.C., Bailey, L.D., Jewgenow, K., 2019. Functional and Morphological Characterization of Small and Large Steroidogenic Luteal Cells From Domestic Cats Before and During Culture. Front Endocrinol (Lausanne) 10, 724.https://doi.org/10.3389/fendo.2019.00724
12. Iborra, R.T.M.-L., A.Castilho, G.Nunes, V. S.Abdalla, D. S.Nakandakare, E. R.Passarelli, M., 2011. Advanced glycation in macrophages induces intracellular accumulation of 7-ketocholesterol and total sterols by decreasing the expression of ABCA-1 and ABCG-1. Lipids in Health and Disease 10(172), 2-7.https://doi.org/10.1186/1476-511X-10-172
13. Kanehisa, M., Araki, M., Goto, S., Hattori, M., Hirakawa, M., Itoh, M., Katayama, T., Kawashima, S., Okuda, S., Tokimatsu, T., Yamanishi, Y., 2008. KEGG for linking genomes to life and the environment. Nucleic Acids Res 36(Database issue), D480-484.https://doi.org/10.1093/nar/gkm882
14. Li, W., Zhi, W., Liu, F., He, Z., Wang, X., Niu, X., 2017. Atractylenolide I restores HO-1 expression and inhibits Ox-LDL-induced VSMCs proliferation, migration and inflammatory responses in vitro. Exp Cell Res 353(1), 26-34.https://doi.org/10.1016/j.yexcr.2017.02.040

15. Li, Y.X., Guo, X., Gulappa, T., Menon, B., Menon, K.M.J., 2019. SREBP Plays a Regulatory Role in LH/hCG Receptor mRNA Expression in Human Granulosa-Lutein Cells. J Clin Endocrinol Metab 104(10), 4783-4792.https://doi.org/10.1210/jc.2019-00913
16. Lindholm, D., Bornhauser, B.C., Korhonen, L., 2009. Mylip makes an Idol turn into regulation of LDL receptor. Cell Mol Life Sci 66(21), 3399-3402.https://doi.org/10.1007/s00018-009-0127-y
17. Long, F., Wang, T., Jia, P., Wang, H., Qing, Y., Xiong, T., He, M., Wang, X., 2017. Anti-Tumor Effects of Atractylenolide-I on Human Ovarian Cancer Cells. Med Sci Monit 23, 571-579.https://doi.org/10.12659/msm.902886
18. Love M I, H.W., Anders S., 2014. Moderated estimation of fold change and dispersion for RNA-seq data with DESeq2. Genome biology 15, 550
19. Luigi Devoto, P.K., Alex Muñoz, Jerome F Strauss 2009 Human corpus luteum physiology and the luteal-phase dysfunction associated with ovarian stimulation. Reproductive BioMedicine Online Vol 18 Suppl.2.https://doi.org/10.1016/s1472-6483(10)60444-0
20. Maher, C.A., Kumar-Sinha, C., Cao, X., Kalyana-Sundaram, S., Han, B., Jing, X., Sam, L., Barrette, T., Palanisamy, N., Chinnaiyan, A.M., 2009. Transcriptome sequencing to detect gene fusions in cancer. Nature 458(7234), 97-101.https://doi.org/10.1038/nature07638
21. Martin M, 2011. Cutadapt removes adapter sequences from high-throughput sequencing reads. Embnet J 17(1), 10–12.https://doi.org/https://doi.org/10 .14806/ej.17.1.200
22. Mesen, T.B., Young, S.L., 2015. Progesterone and the luteal phase: a requisite to reproduction. Obstet Gynecol Clin North Am 42(1), 135-151.https://doi.org/10.1016/j.ogc.2014.10.003
23. Miranda-Jimenez, L., Murphy, B.D., 2007. Lipoprotein receptor expression during luteinization of the ovarian follicle. Am J Physiol Endocrinol Metab 293(4), E1053-1061.https://doi.org/10.1152/ajpendo.00554.2006
24. Nardo, L.G., Sallam, H.N., 2006. Progesterone supplementation to prevent recurrent miscarriage and to reduce implantation failure in assisted reproduction cycles. Reprod Biomed Online 13(1), 47-57.https://doi.org/10.1016/s1472-6483(10)62015-9
25. Niswender, G.D., Juengel, J.L., Silva, P.J., Rollyson, M.K., McIntush, E.W., 2000. Mechanisms controlling the function and life span of the corpus luteum. Physiol Rev 80(1), 1-29.https://doi.org/10.1152/physrev.2000.80.1.1
26. Richards, J.S., Pangas, S.A., 2010. The ovary: basic biology and clinical implications. J Clin Invest 120(4), 963-972.https://doi.org/10.1172/JCI41350
27. Shimano, H., Sato, R., 2017. SREBP-regulated lipid metabolism: convergent physiology - divergent pathophysiology. Nat Rev Endocrinol 13(12), 710-730.https://doi.org/10.1038/nrendo.2017.91
28. Song, H.P., Hou, X.Q., Li, R.Y., Yu, R., Li, X., Zhou, S.N., Huang, H.Y., Cai, X., Zhou, C., 2017. Atractylenolide I stimulates intestinal epithelial repair through polyamine-mediated Ca(2+) signaling pathway. Phytomedicine 28, 27-35.https://doi.org/10.1016/j.phymed.2017.03.001
29. Stocco, C., Telleria, C,Gibori, G., 2007. The molecular control of corpus luteum formation, function, and regression. Endocr Rev 28(1), 117-149.https://doi.org/10.1210/er.2006-0022

30. Vannuccini, S., Bocchi, C., Severi, F.M., Challis, J.R., Petraglia, F., 2016. Endocrinology of human parturition. Annales d\"Endocrinologie, S0003426616300427
31. Wang, H., Humbatova, A., Liu, Y., Qin, W., Lee, M., 2020. Mutations in SREBF1, Encoding Sterol Regulatory Element Binding Transcription Factor 1, Cause Autosomal-Dominant IFAP Syndrome. The American Journal of Human Genetics 107(1), 34-45.https://doi.org/10.1016/j.ajhg.2020.05.006
32. Wiktorowska-Owczarek, A., Berezinska, M., Nowak, J.Z., 2015. PUFAs: Structures, Metabolism and Functions. Adv Clin Exp Med 24(6), 931-941.https://doi.org/10.17219/acem/31243
33. Woollett, L.A., 2008. Where does fetal and embryonic cholesterol originate and what does it do? Annu Rev Nutr 28, 97-114.https://doi.org/10.1146/annurev.nutr.26.061505.111311
34. Zhu, B., Zhang, Q.L., Hua, J.W., Cheng, W.L., Qin, L.P., 2018. The traditional uses, phytochemistry, and pharmacology of Atractylodes macrocephala Koidz.: A review. J Ethnopharmacol 226, 143-167.https://doi.org/10.1016/j.jep.2018.08.023

Tables

Table 1
Statistical summary analysis of RNA-seq data sets of treated cells and control cells

Sample	Means for raw reads			Means for mapping		
	No. of raw reads	No. of valid reads	Q20 (%)	No. of map reads	No. of unique mapped reads	Uniquely mapped ratio (%)
Control cells	52,950,059	52,340,848	98.03	51,014,192	48,058,826	91.82
Treated cells	58,841,865	58,189,124	98.24	56,730,426	53,563,083	92.06

Table 2
Significantly upregulated or downregulated genes involved in signaling in FOGCs.

Gene name	Gene Description	Fold Change	*P* adjust	Regulation
ABCA1	ATP binding cassette subfamily A member 1	4.554	0.000006	up
SCD	stearoyl-CoA desaturase	2.48	0.003099	up
LDLR	low density lipoprotein receptor	1.934	0.025723	up
CYP1A1	cytochrome P450 1A1	0.451	0.026415	down
FADS2	fatty acid desaturase 2	1.609	0.034371	up
ABCG1	ATP binding cassette subfamily G member 1	3.724	0.044671	up
SREBF1	sterol regulatory element binding transcription factor 1	1.839	0.040339	up
StAR	steroidogenic acute regulatory protein	1.48	0.042111	up
MYLIP	myosin regulatory light chain interacting protein	2.451	0.002304	up

Table 3
Primers for RT-qPCR.

Gene Name	Nucleotide sequence (5'-3')
GAPDH	Forward CAAGGCTGTGGGCAAGGTCATC
	Reverse TTCTCCAGGCGGCAGGTCAG
SREBF1	Forward GGCATCGCAAGCAGGCTGAC
	Reverse GGTGGGAGGTGGGCAGTGG
ABCG1	Forward ACATGCTGTTGCCACACCTCAC
	Reverse TCCTGCCTTCGTCCTTCTCCTG
ABCA1	Forward GGCAACGGCACTGAGGAAGATG
	Reverse TGCGGGAAAGAGGACTGGACTC
LDLR	Forward GCCAGCAGAGGAGACGAGGAG
	Reverse CCCGAAGCCCAGGAGGATGAG
SCD	Forward AAATTCCCTTCGGCCAATGAC
	Reverse TCTCACCTCCTCTTGCAGCAA
CYP1A1	Forward TGGCACCATCAACAAGGCACTG
	Reverse AAAGACCTCCAAGCGGGCAATG
FADS2	Forward GGATATGCGGGCGTAGAAGC
	Reverse GTGCCGTGCAAATAGGTGGA
StAR	Forward GTGGAGCACATGGAAGCGATGG
	Reverse GCAGCCAACTCGTGGGTGATG
MYLIP	Forward AACGAGGGAGCAGGGTTGAA
	Reverse ACACTGCCGAGACAGAGGTT

Figures

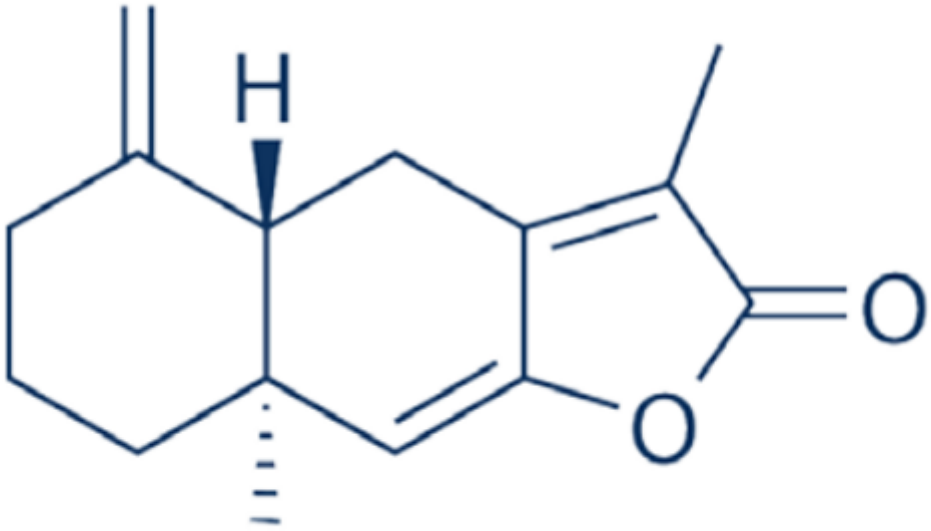

Figure 1

Chemical structure of Atractylenolide-I (AT-I).

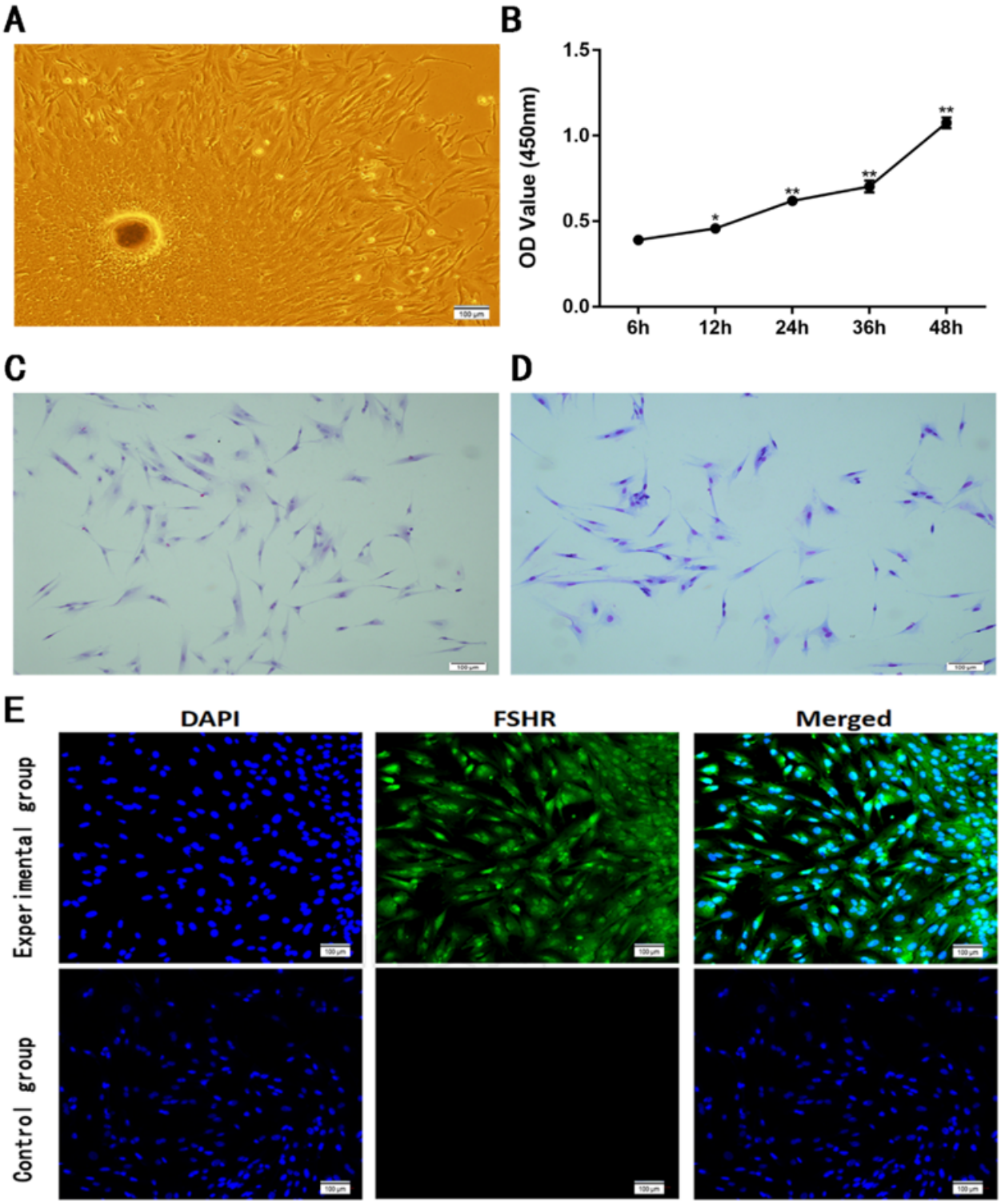

Figure 2

Morphological observation and growth curve of the primary FOGCs. (A)The primary FOGCs attach to the substrate around the oocytes and begin to display an elongated or fibroblastic property within the first 24 h of culture. (B) Growth curve of cultivated cells within 48 h. (C) The HE staining of cultivated cells on substrate. (D) The Giemsa staining of cultivated cells on substrate. (E) Immunofluorescence of cultivated

cells on substrate: FSHR (green) as the marker expressed in FOGCs, negative-control group and nuclei with DAPI staining (blue). Values are expressed as mean±S.D. (n=4). *,$P < 0.05$; **,$P < 0.01$.

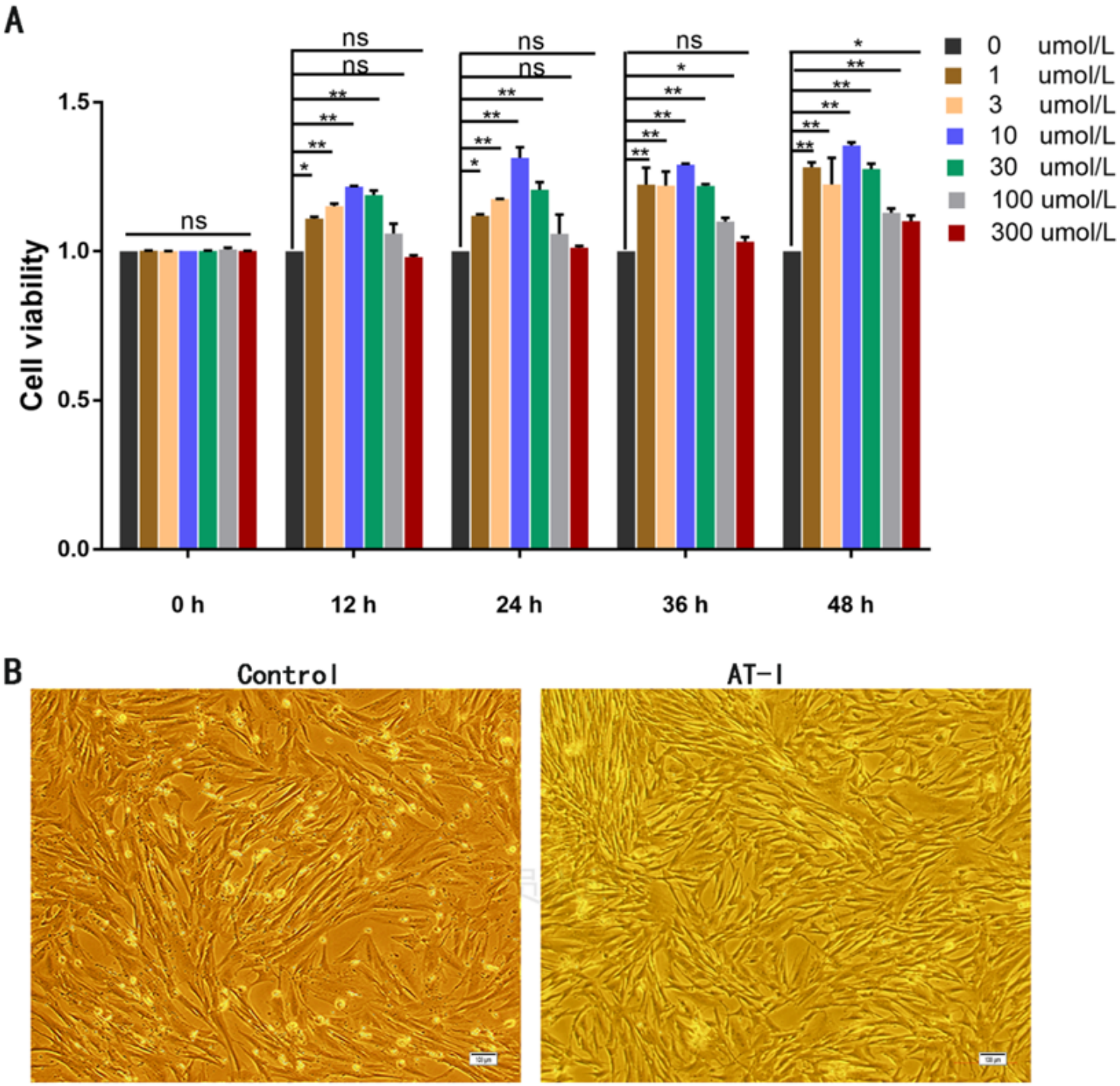

Figure 3

Effect of AT-I on the FOGCs. (A) Treatment with AT-I in 1, 3, 10 and 30 μmol/L could effectively promote FOGCs proliferation from 12 h to 48 h ;100 μmol/L significantly increased FOGCs proliferation after 36 h and the increased effect of 300 μmol/L happened at 48 h (P<0.05). (B) After 10umol/L AT-I treated 36

hours, the density of granulosa cells increased, cell viability increased significantly. Values are expressed as mean±S.D. (n=4). *,P < 0.05; **,P <0.01; ns, not statistically significant.

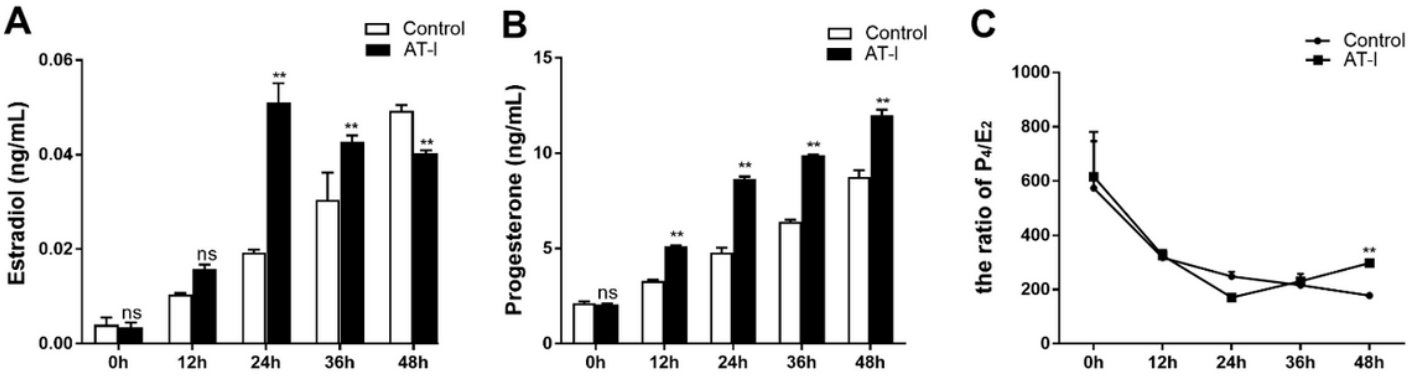

Figure 4

The effect of 10 umol/L AT-I on the synthesis of E_2 and P_4 in FOGCs. (A) AT-I could significantly promote the E_2 secretion in FOGCs at 24 h and 36 h, while the increased tendency weakened at 48 h. (B) The P_4 concentration significantly increased by AT-I treatment from 12 h to 48 h. (C) The ratio of P_4/E_2 indicated that the E_2 secretion was more obviously than P_4 secretion in FOGCs within 36 h after AT-I treatment. However, the secretion pattern of E_2 and P_4 changed at 48 h, in which the FOGCs secret P_4 more obviously than that E_2 secretion. Values are expressed as mean±S.D. (n=3). *,$P < 0.05$; **,$P <0.01$; ns, not statistically significant.

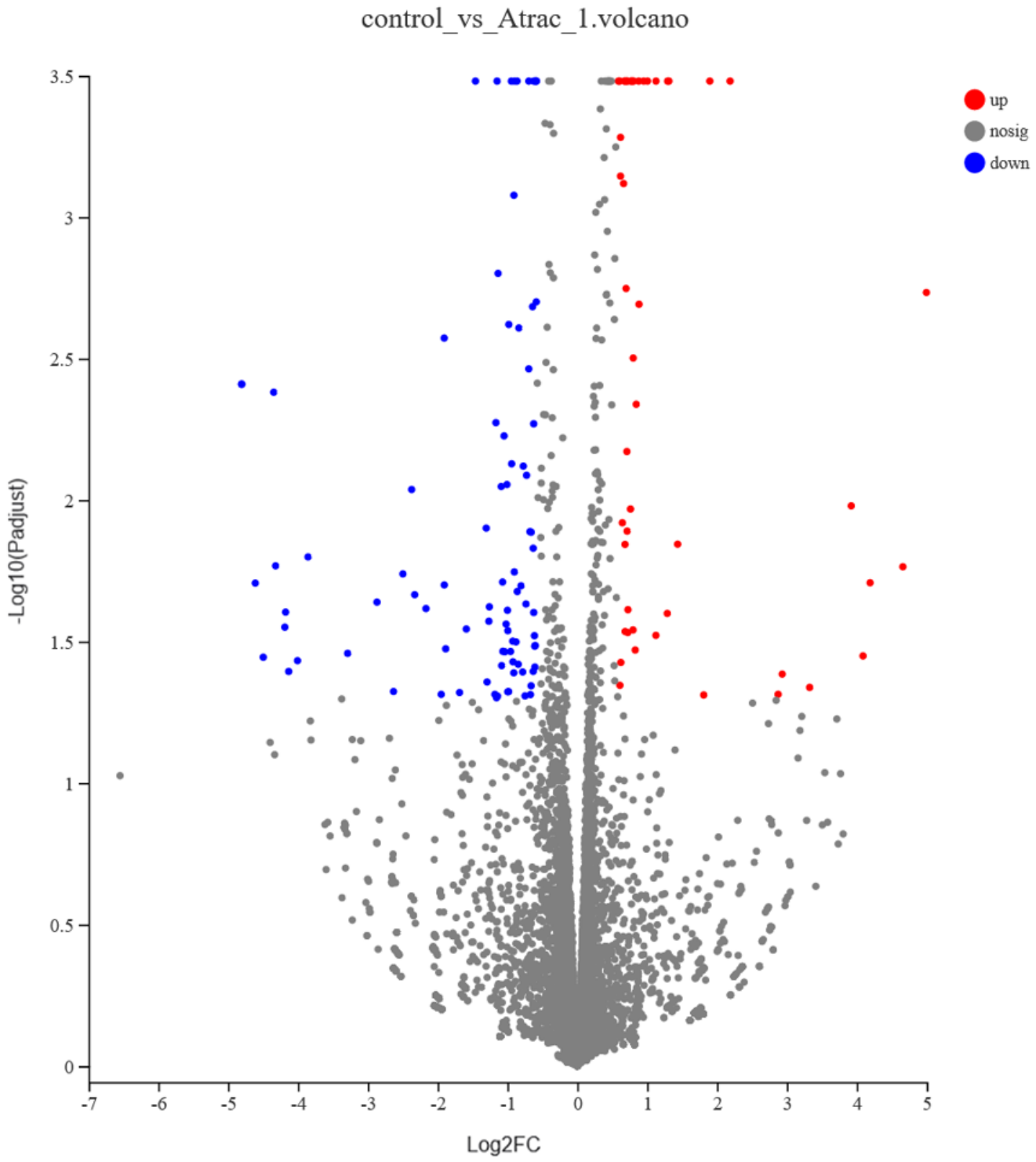

Figure 5

Volcano graph of 137 differentially expressed genes between two groups. Red represents upregulated DEGs; blue represents downregulated DEGs.

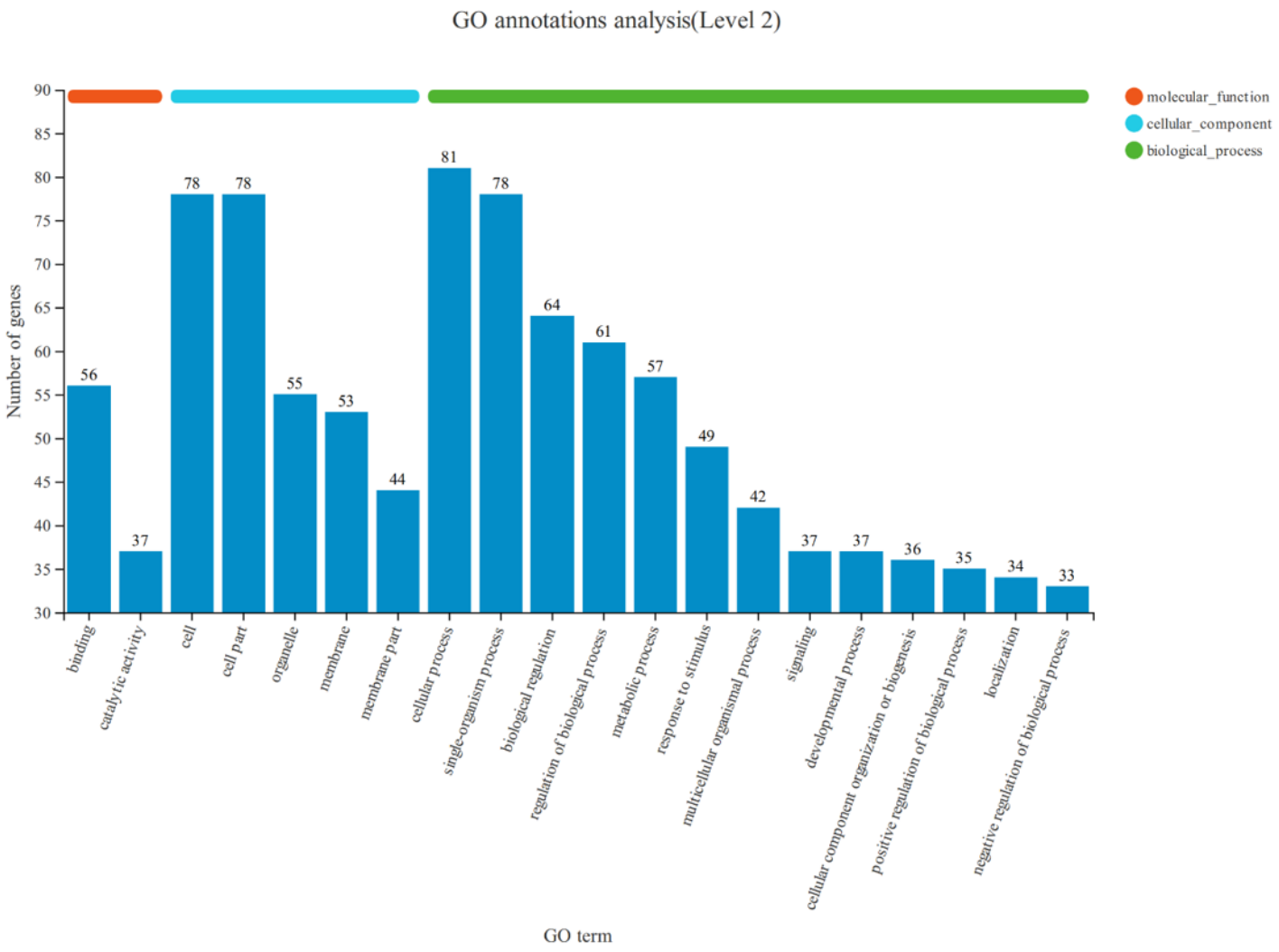

Figure 6

GO classifications of genes in FOGCs. The abscissa is the GO classification, and the ordinate is the number of genes in each category.

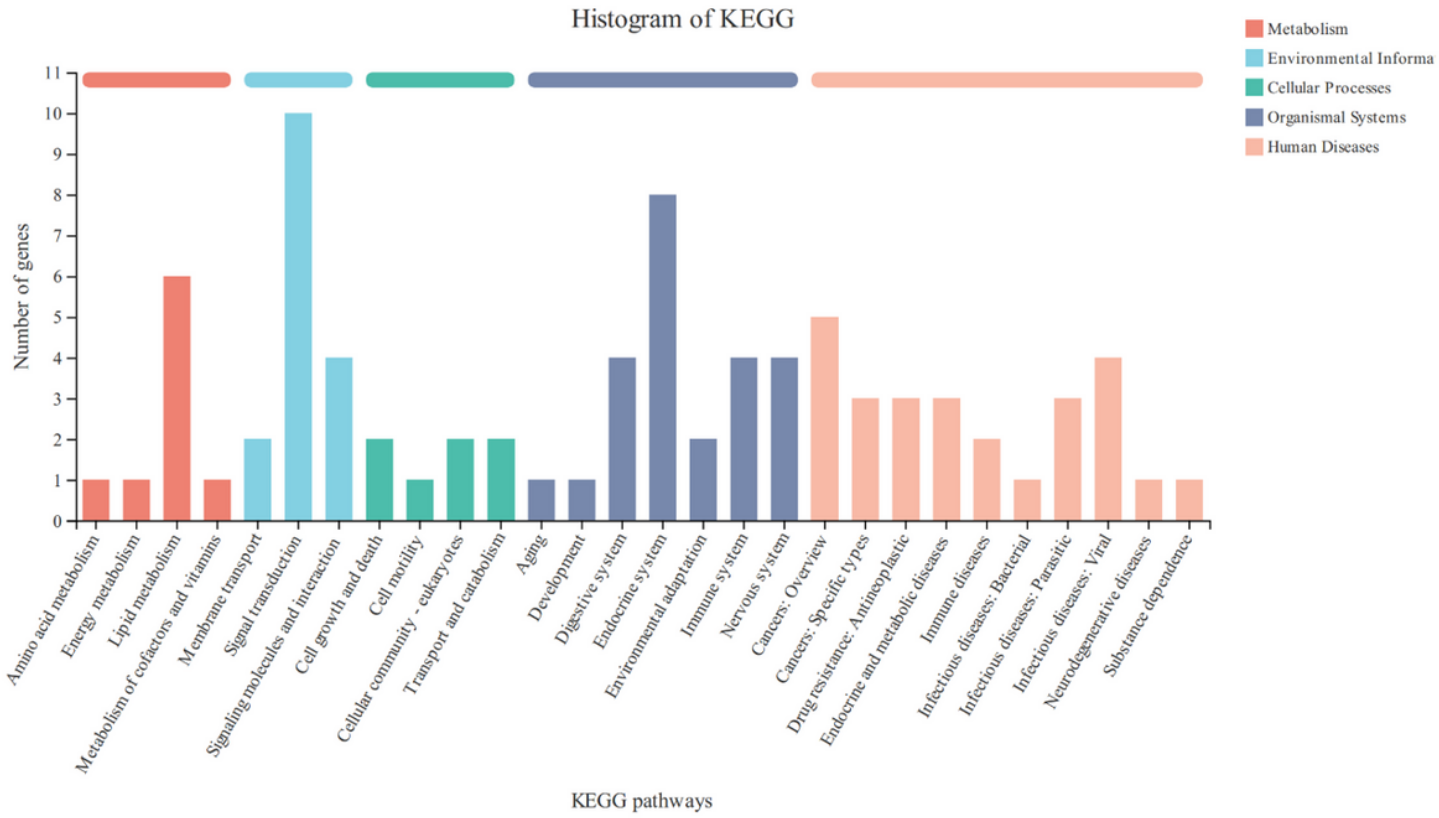

Figure 7

KEGG pathway classification of genes in FOGCs. The abscissa is the name of the KEGG metabolic pathway, and the ordinate is the ratio of the number of genes annotated to the pathway and the number of genes in the annotated genes.

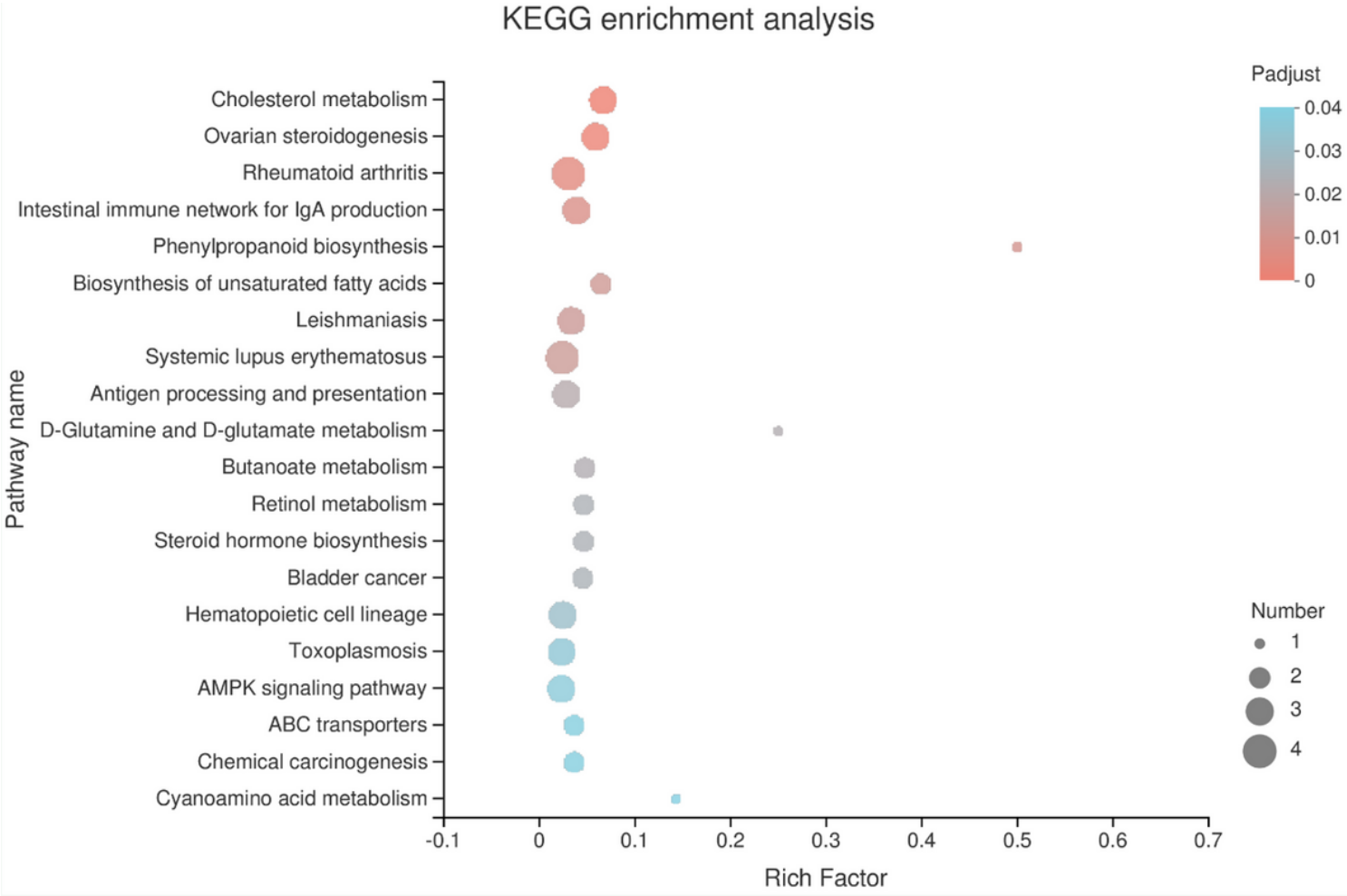

Figure 8

The significantly enriched KEGG pathway of DEGs. Rich factor, number of differentially expressed genes/total number of genes in this KEGG pathway. The larger the value, the greater the enrichment.

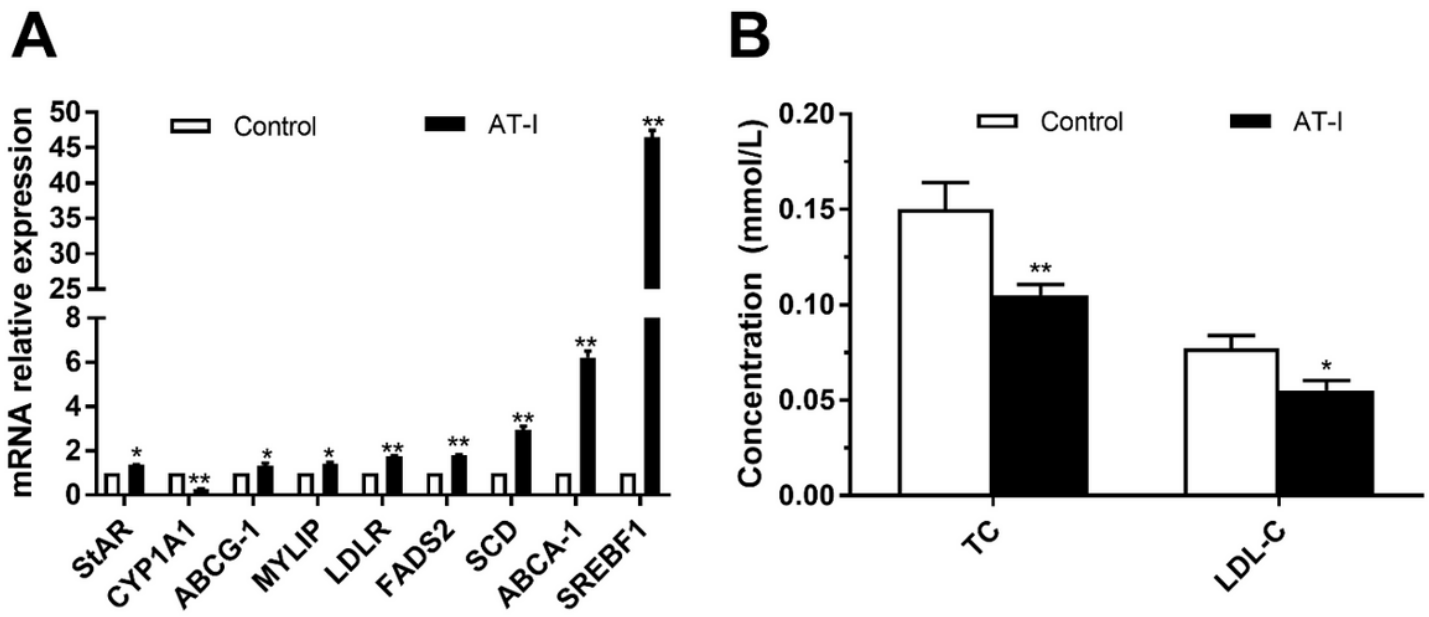

Figure 9

Verification of transcriptome results (A) Relative quantification of DEGs by RT-qPCR. The expression of each gene was normalized to the average expression of the endogenous reference gene GAPDH. (B) Biochemical verification. After AT-I treatment, the contents of total cholesterol and LDL-cholesterol both declined. The values are expressed as mean±S.D. (n=3). *P < 0.05; **P<0.01; ns, not statistically significant.